DRAFT VERSION 2 JULY 2007
Preprint typeset using LaTeX style emulateapj v. 5/14/03

IMPLICATIONS FOR THE ORIGIN OF GRB070201 FROM LIGO OBSERVATIONS
LIGO-P070081-02-Z FOR INTERNAL DISTRIBUTION ONLY - UNREVIEWED DRAFT

THE LSC

(Dated: RCS ; compiled 2 July 2007)
Draft version 2 July 2007

ABSTRACT

We analyzed LIGO data coincident with GRB070201, a short hard GRB whose electromagnetically-determined sky position could include the spiral arms of M31 (the Andromeda galaxy). Compact binary inspirals and soft γ-ray repeaters were identified as possible progenitors; both are possible sources of strong gravitational radiation. No plausible gravitational wave candidates were found within a 180 s window around the time of GRB070201. We estimate that LIGO would have detected gravitational waves from an inspiraling compact binary in M31 (with $> 99\%$ confidence) at the time of this GRB. Therefore GRB070201 did not arise from a compact binary merger in M31. Indeed, if GRB070201 was caused by a binary neutron star merger, we find that $D < 5$ Mpc is excluded for 1-3 $M_\odot$/1-3 $M_\odot$ systems assuming random inclination at 90% confidence. Allowing for other progenitors, we searched for unmodeled gravitational wave burst signatures via two-detector correlations. The result implies that a gravitational wave burst with characteristic frequency f 150Hz from GRB070201 most probably emitted less than $3 \times 10^{-4} M_\odot$ in any 100ms long time interval of the signal region if the source was in M31 and emitted its waves at the same frequency as LIGO's peak sensitivity. This upper limit does not exclude current models of SGRs at the M31 distance.

Subject headings: gamma-ray bursts – gravitational waves – compact object mergers – soft gamma-ray repeaters

1. INTRODUCTION

Gamma ray bursts (GRBs) are intense flashes of γ-rays which are observed to be isotropically distributed over the sky (see, e.g.: Piran 2005; Meszaros 2002, and references therein). The short time variability of the sources indicates that they are very compact. Combined observations, using γ-ray and x-ray satellites such as Vela, BATSE, BeppoSax, Swift, Konus-Wind, and INTEGRAL (see Klebesadel et al. (1973), Meegan et al. (1992), Paciesas et al. (1999), Frontera et al. (2000), Mazets and Golenetskii (1981), Gehrels et al. (2004), and references therein), with follow-up by optical and radio telescopes of the region around GRBs eventually yielded the direct observation of the afterglow. In turn, host galaxies were identified for some GRBs and their distances measured. Together these observations imply that typical GRBs are of cosmological origin. Two types of GRBs are distinguished by their characteristic duration (see Kouveliotou et al. (1993); Gehrels et al. (2006)).

Long GRBs have duration $\gtrsim 2$ s. Detailed observations of long GRBs demonstrate their association with star-forming galaxies ranging up to a redshift of $z \simeq 6.3$ [see Watson et al. (2006), Jakobsson et al. (2006), and references therein]. Futhermore, several nearby long GRBs have been spatially and temporally coincident with supernovae (e.g. Campana et al. 2006; Hjorth et al. 2003; Galama et al. 1998).

Short GRBs have duration $\lesssim 2$ s. The progenitors of short GRBs are not so well understood. While there are associations with distant galaxies of many different types and different star formation histories , there is at least one powerful burst from a known Galactic source, SGR1806-20 (Nakar et al. 2006; Hurley et al. 2005)). An attempt to associate all short GRBs with soft γ-ray repeaters (SGRs) suggested only about 15% of them can be accounted for in this way (Nakar et al. 2006). Moreover, the spectral characteristics and energetics of other observed short GRB events and their follow-up afterglows seem to contradict this theory in most cases (Nakar et al. 2006). The current leading hypothesis to explain most short GRBs is the merger of neutron star or neutron star–black hole binaries (see for example Nakar (2007) and references therein). No observations have definitively confirmed the association between short GRBs and binary mergers.

It is therefore plausible that GRB central engines are also strong gravitational wave (GW) emitters at frequencies accessible to ground-based detectors like LIGO, GEO, and Virgo (Abbott and et al 2005; Kochanek and Piran 1993; LIGO Scientific Collaboration 2006, 2005; Finn et al. 2004). Bursts of gravitational waves are expected to be emitted during the GRB event, with a characteristic duration comparable to that of the associated GRB, though the amplitude and frequency spectrum of the gravitational-wave burst are unknown. In the case of short GRBs produced by compact binary mergers, gravitational waves with relatively well modelled amplitude and frequency evolution will be emitted during the inspiral phase of the binary preceding the event that produces the GRB.

GRB070201 was an intense, short, hard GRB detected by Konus-Wind and INTEGRAL (SPI-ACS); it was also observed by Swift (BAT) but with a high-intensity background as the satellite was entering the South Atlantic Anomaly (GCN Circular #6088). The burst light-curve exhibited a multi-peaked pulse with duration ~ 0.15 s, followed by a much weaker, softer pulse that lasted ~ 0.08 s. Using early reports, Perley and Bloom (GCN #6091) pointed out that the location annulus of the event intersected the outer spiral arms of M31. A modified error box, centered 1.1 degrees from the center of M31 with an area of 0.325 square degrees, was later reported (GCN #6103) by including data from MESSENGER

(GCN #6098). This error box overlaps the spiral arms of M31. Based on the Konus-Wind observations (GCN #6094), the burst had a fluence of $1.57(-0.21,+0.06) \times 10^{-5}$ erg cm^{-2} in the 20 keV – 1 MeV range. The authors pointed out that if the burst source were actually located in M31 (at a distance of only $\simeq 770$ kpc) the isotropic energy release would be $\sim 10^{45}$ erg, comparable to the energy release in giant flares of soft gamma-ray repeaters: e.g., the 5$^{\rm th}$ March 1979 event from SGR 0526-66 ($\sim 2 \times 10^{44}$ erg in the initial pulse) and the 27$^{\rm th}$ December 2004 event from SGR 1806-20 ($\sim 2 \times 10^{46}$ erg). Conversely if the event had an isotropic energy release more typical of short hard GRBs, e.g., $\sim 10^{48} - 10^{52}$ erg (Berger 2007), then it would have to be located at least ~ 30 times further than M31 (i.e., further than ~ 23 Mpc).

At the time of the GRB070201, the Hanford detectors of the Laser Interferometer gravitational wave Observatory (LIGO) Abbott et al. (2004) were stable and recording science quality data, while the LIGO Livingston and Virgo Acernese et al. (2006) detectors were not taking data The LIGO data around GRB070201 was searched for evidence of a gravitational wave signal from compact binary inspiral or the central engine of the GRB itself.

A standard measure of the sensitivity of a detector to gravitational waves is the distance to which an optimally positioned and oriented double neutron star binary would produce a response in our data stream that, when optimally filtered for the inspiral waves, peaks at a signal to noise ratio of 8 (see,e.g. LIGO Scientific Collaboration 2005, and references therein). At the time of GRB070201, this distance was 43.3 Mpc and 15.4 Mpc for the Hanford 4km and 2km detectors, respectively. However, the sensitivity of a detector to a gravitational wave depends on the location of the source on the sky and on the polarization angle of the waves. (In the case of compact binaries, it also depends on the inclination angle of the orbital plane relative to the line of sight.) At the time of GRB070201, reach in the direction of M31 (averaged over polarization angle) is only about 30% of this maximum. More details of the instrumental sensitivity can be found in Sec. 2.

The search for gravitational waves from a compact binary inspiral focused on objects with masses in the ranges $1M_\odot \leq m_1 \leq 40M_\odot$ and $1M_\odot \leq m_2 \leq 3M_\odot$. The core of the search is matched filtering, cross-correlating the data with the expected gravitational waveform for binary inspiral and uses methods reported previously (see,e.g LIGO Scientific Collaboration 2005, and references therein) Section 3 provides more details. Uncertainties in the expected waveforms can lead to decreased sensitivity of the search to the gravitational wave signal from the inspiral phase; this is particularly true of systems with higher masses and systems with substantial spin (Grandclement et al. 2003).This is accounted for by studying the dependence of sensitivity of the search to a variety of model waveforms based on different approximation methods.No plausible gravitational wave candidates were identified in this search. The result is interpreted to exclude a compact binary progenitor in M31 (with $> 99\%$ confidence) at the time of GRB070201.

The search for gravitational waves from the central engine itself is based on cross-correlating data from two detectors and does not make use of a specific model for the gravitational wave signal. This is an appropriate method when the gravitational wave signal is not well modeled theoretically, such as signals from the actual merger of a compact binary or a supernova explosion.

The remainder of the paper is organized as follows. In section 2, we discuss the LIGO detectors and the data taken around the time of GRB070201. In section 3, we report on the inspiral gravitational wave search, briefly reviewing the methods and algorithms used, and concluding with the astrophysical implications of the search for the GRB070201 event. In section 4, we report on the search for other gravitational wave bursts and present the astrophysical implications of that search. Since no plausible gravitational wave signal was detected above the background either in the inspiral or the burst search, we present the astrophysical implications of these results on the understanding of short GRBs in section 5.

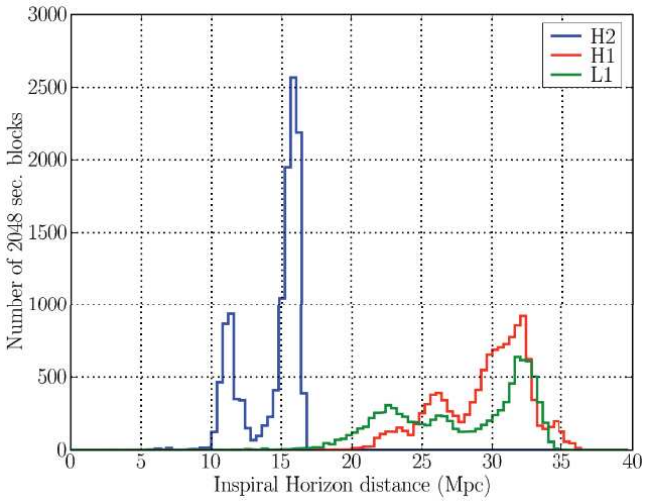

FIG. 1.— For the first calendar year of LIGO's fifth science run (S5), a histogram of the inspiral horizon distance, the maximum distance to which a single detector is sensitive to the binary inspiral of two 1.4 $M_\odot$ neutron stars (with optimal orientation and sky position). The vertical axis has units of time measured in 2048 second long blocks.

2. LIGO OBSERVATIONS

LIGO is comprised of three instruments at two geographically distinct locations (a 4 km and a 2 km at Hanford Observatory, refered to as detectors H1 and H2, and a 4 km at Livingston Observatory, refered to as detector L1). As of Summer 2007, all three LIGO detectors are operating at design sensitivity **[ref:DCC-060009-02]**. The fifth science run (S5) started on November 4th, 2005 and is scheduled to end after one year of integrated coincidence data are collected.

The LIGO detectors use suspended mirrors at the ends of kilometer-scale, orthogonal arms to form a Michelson interferometer with Fabry-Perot arms. A gravitational wave induces a time-dependent strain $h(t)$ on the detector. While acquiring scientific data, feedback to the mirror positions and to the laser frequency keeps the optical cavities near resonance, so that interference in the light from the two arms recombining at the beam splitter depends on the difference between the lengths of the two arms. A photodiode senses the light, and a digitized signal is recorded at a sampling rate of 16384 Hz.

The LIGO detectors have a sensitive frequency bandwidth ~ 1000 Hz, with a minimum at ≈ 120 Hz, which is truncated at low frequencies by seismic noise and at high frequencies by laser shot noise. In addition, environmental disturbances, control systems noise, and many other noise sources result in a non-stationary and non-Gaussian background.

2.1. *LIGO Observations Coincident with GRB070201*

At the time of the GRB trigger, both LIGO Hanford detectors were stable and recording science quality data, while the LIGO Livingston and VIRGO detectors were not taking data. The Hanford detectors had been in science mode for more than 14 hours before the GRB trigger, and stayed in science mode for more than 8 hours after the GRB trigger, providing ample data for background studies.

An asymmetric 180 seconds long *on-source* segment, $-120/+60$ s about the GRB trigger time, was searched for gravitational wave signals. This traditional choice is conservative enough to accommodate inspiral type signals, trigger time ambiguities and theoretical uncertainties. The significance of candidate events was evaluated using studies covering several hours of *off-source* data from the same science mode stretch outside of, but near to, the on-source segment.

The ideal response of a detector to an incident gravitational wave is a weighted combination of the two underlying gravitational wave polarizations denoted by $h_+(t)$ and $h_\times(t)$:

$$h(t) = F_+(\theta,\phi,\psi)h_+(t) + F_\times(\theta,\phi,\psi)h_\times(t)\,. \quad (1)$$

The dimensionless weighting amplitudes, or *antenna factors*, F_+ and $F_\times$ depend on the position (θ,ϕ) of the source relative to the detector and ψ is the gravitational wave polarization angle. For GRB070201, localized near to M31, the Hanford root-mean-square (RMS) antenna factor, F_{RMS}, was

$$F_{RMS} = \sqrt{F_+^2 + F_\times^2}/\sqrt{2} = 0.304 \quad (2)$$

a combination which does not depend on the polarization angle ψ. Despite the sub-optimal location of GRB070201 for the LIGO Hanford detectors, they still had significant sensitivity for the polarization states compatible with the detector.

2.2. *Data Quality for the Times Surrounding the GRB070201 Trigger*

A suite of data quality tests are applied to LIGO data (LIGO Scientific Collaboration XXX). No anomalous behavior was found in either instrument at the time of GRB070201. On the other hand, a number of data quality issues were identified in the off-source time used for background estimation (which amounted to 60084s, or 16.7 hrs). Triggers were excluded from 530 s of coincident, off-source data so identified, or 0.9% of the off-source time.

Overflows in digital signals used in the feedback control systems were responsible for 29 s in H1 and 29 s in H2 of excluded time. Seismic noise in the 3–10 Hz band known to produce triggers in H1 was used to veto 160 s of data. Disturbances that produced a loss in power in the H2 detector arm cavities larger than 4% were also vetoed, amounting to 163 s, which include 11 s when there were overflows in H2. No such fluctuations in arm power were observed in H1. Finally, 160 s were used to apply hardware injections.

3. SEARCH FOR GRAVITATIONAL WAVES FROM A COMPACT BINARY PROGENITOR

A number of searches for gravitational waves from compact binaries have been completed on the LIGO data (Abbott et al. 2005a, 2006, 2005b, 2007). The same search methods were applied to the on-source time around GRB070201 (LIGO Scientific Collaboration 2007a). In this section we briefly discuss the search methods, report the results of the search, and discuss their interpretation.

3.1. *Search Method*

The core of the inspiral search involves correlating the LIGO data against the theoretical waveforms expected from compact binary coalescence; i.e., matched filtering the data (Wainstein and Zubakov 1962). The gravitational waves from the inspiral phase, when the binary orbit tightens under GW emission prior to merger, are accurately modeled in the band of LIGO sensitivity for a wide range of binary masses (Blanchet et al. 1995; **?**). The expected gravitational-wave signal, as measured by LIGO, depends on the masses and spins of the binary elements, as well as the spatial location, inclination and GW polarization angle. In general, the power of matched filtering depends most sensitively on accurately tracking the phase evolution of the signal. The phasing of compact binary inspiral signals depends on the masses and spins, the time of merger, and an overall phase. In a search for gravitational waves from compact binaries, one therefore uses a discrete set of *template waveforms* against which the data is correlated.

In this search, we adopt template waveforms which span a two-dimensional parameter space (one for each component mass) such that the maximum loss in signal-to-noise (SNR) for a binary with negligible spins would be 3%. While the spin is ignored in the template waveforms, we show below that the search is still sensitive to binaries with most physically reasonable spin orientations and magnitudes with only moderate loss in sensitivity. To generate a γ-ray burst, at least one of the objects in a compact binary must be a material object, probably a neutron star, while the second object must either be a neutron star or a stellar mass black hole with low enough mass (Vallisneri 2000; Rantsiou et al. 2007) to cause disruption of the neutron star before it is swallowed by the hole. The mass-parameter space covered by the templates is therefore $1M_\odot < m_1 < 3M_\odot$ and $1M_\odot < m_2 < 40M_\odot$. The number of template waveforms required to achieve this coverage depends on the detector noise curve; at the time of the GRB, 7171 and 5417 templates were required in H1 and H2, respectively.

The data from each of the LIGO instruments is filtered through the bank of templates. If the matched filter signal-to-noise exceeds a threshold $\rho*$, the template masses and the time of the maximum signal-to-noise are recorded. For a given template, threshold crossings are clustered using a sliding window equal to the duration of the template as explained in (Allen et al. 2005). For each trigger identified in this way, the coalescence phase and the effective distance to the source (assuming masses to be those of the template) are also computed. Triggers identified in each instrument are further required to be coincident in the time and mass parameters between the two operating instruments taking into account the correlations between those parameters. This significantly reduces the number of background triggers that arise from matched filtering in each instrument independently. Because H1 was more sensitive than H2, two different thresholds were used in the matched filtering step: $\rho^* = 5.5$ in H1 and $\rho^* = 4.0$ in H2. This choice takes advantage of the better sensitivity in H1 while still using H2 to reduce the rate of accidentals.

To further reduce the background, two more signal-based tests are applied to the data. First, a χ^2-veto (Allen 2005), which measures the quality of the match between the data and the template, is computed; triggers with large χ^2 values are discarded. Second, the r^2 veto (Rodriguez 2007), which looks

at the time the χ^2 statistic stays above a certain threshold, is also used to reduce the background. The SNR and χ^2 from a single detector are combined into an effective signal-to-noise ρ_{eff} (Abbott et al. 2007), and the effective SNRs from the two detectors are combined in quadrature to form a single quantity ρ^2_{eff} which provides good separation between signal candidate events and background.

The final list of coincident triggers are then called *candidate events*.

3.2. *Background and results*

Gravitational-wave detectors are susceptible to many sources of environmental and intrinsic noise. These sources often result in non-Gaussian and non-stationary noise backgrounds. To estimate the background in this search, an equal number of 180 s off-source segments were selected to the past and future of the γ-ray trigger. All of the data, including the on-source segment, was analyzed using the methods described above. Triggers arising from the on-source segment were then removed, as were triggers within bad-quality segments, leading to an estimate of the number of accidental triggers per 180s segment. A total off-source time of 58500 s was analyzed, corresponding to 325 segments each of 180 s. The mean rate of coincidences was 2.7 per 180 s segment.

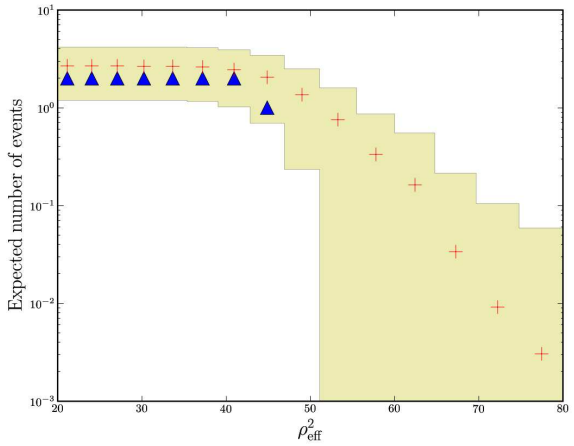

FIG. 2.— A cumulative histogram of the coincident triggers in the on-source time (triangles) overlaid on the expected number of background triggers based on the analysis of the off-source times (pluses) as a function of the effective signal-to-noise ratio (Abbott et al. 2007). The shaded region indicates the 1σ variation in the background estimate observed in the off-source times. The figure shows that the observed number of on-source triggers is consistent with the estimation for the background.

Figure 2 shows the cumulative histogram of the coincident triggers in the on-source time overlaid on the expected number of triggers based on the analysis of the off-source times as a function of the effective signal-to-noise ratio Abbott et al. (2007). Two candidates were observed in the on-source time. The loudest on-source candidate had effective signal-to-noise $\rho_{\rm max} = 6.9$ and the probability of a background event with effective signal-to-noise $\rho_{\rm eff} > \rho_{\rm max}$ is estimated to be about 85% based on the off-source distribution. For completeness, both of these triggers in the on-source time were examined using an a posteriori analysis. No plausible gravitational wave signals from compact binary coalescence were identified around the time of GRB070201.

3.3. *Astrophysical interpretation*

The observations reported here can be used to constrain the distance to the GRB by computing the probability that the largest signal-to-noise in the on-source time would be less than or equal to that observed given the presence of a compact binary progenitor. Denote the gravitational-wave signal $h(t;m_1,D,\vec{\mu})$ where m_1 is the mass of the more massive object, D is the physical distance to the binary, and $\vec{\mu} = \{m_2, \vec{s_1}, \vec{s_2}, \iota, \Phi_0, t_0\}$ is the mass of the less massive object, the spins, the inclination, the coalescence phase, and the coalescence time. The probability of interest is then

$$p[\text{All events have } \rho \leq \rho_{\rm max}|h(t;m_1,D)] = \int p(\vec{\mu}) p[\text{All events have } \rho \leq \rho_{\rm max}|h(t;m_1,D,\vec{\mu})] d\vec{\mu} \quad (3)$$

where the nuisance parameters $\vec{\mu}$ are integrated over some prior distribution $p(\vec{\mu})$. This integration was performed by injecting simulated signals into the data streams of both detectors according to the desired prior distribution, and evaluating the efficiency for recovering those injections as candidate events (as described in Sec. 3.1), as a function of m_1 and D. We choose uniform priors over m_2, Φ_0, and t_0.

Astrophysical black holes are expected to have substantial spin. The maximum allowed by accretion spin-up of the hole is $(a/M) = (cS/GM^2) < 0.9982$ (Thorne 1974) in units of the Kerr spin parameter (S is the spin angular momentum of the black hole). More detailed simulations and recent observations provide a broad range of values with a maximum observed spin $(a/M) > 0.98$ **?**. The maximum spin that a neutron star can have is estimated from a combination of simulations and observations of pulsar periods. Numerical simulations of rapidly spinning neutron stars give $(a/M) < 0.75$ (Cook et al. 1994), the maximal spin of the observed pulsar sample may be substantially lower than that. In our simulations, we adopted a distribution in which the spin magnitudes are uniformly distributed between zero and $(a/M) = (cS/GM^2) < 0.9982$ and $(a/M) = (cS/GM^2) < 0.75$ for the black holes and neutron stars respectively, while the direction of each spin is uniform over the sphere.

There is strong evidence that γ-ray bursts are beamed (see,e.g., Nakar 2007; Soderberg et al. 2006; Grupe et al. 2006, and references therein). If this is the case, the most likely direction for beaming is along the total angular momentum vector of the system. For binaries with small component spins, this will correspond to the direction orthogonal to the plane of the orbit. Hence the inclination angle of the binary, relative to the line of sight, is most likely to be close to zero. Since zero inclination is the best case for detection of gravitational waves, we report results for a uniform prior on $\cos\iota$ which provides a conservative constraint.

A number of systematic uncertainties enter into this analysis: calibration and Monte-Carlo statistics have the largest effects. These uncertainties are folded in by marginalizing over their effects in a manner similar to that described in Abbott et al. (2007).

Electromagnetic observations of GRB070201 localized the event to an error box covering the outer edges of Andromeda. Setting $D = D_{\rm M31} = 770$ kpc, we exclude a compact binary progenitor in Andromeda at the $> 99\%$ level. In particular, a compact binary progenitor, with masses $m_1 = 1.4 M_\odot$ and $m_2 = 10.0 M_\odot$, located in Andromeda would be excluded at the $\simeq 99.6\%$ level.

Figure 3 shows the contours of constant probability

p[All events have $\rho \leq \rho_{\rm max}|h(t;m_1,D)$]. Compact binaries corresponding to parameters (m_1, D) in the shaded region are excluded as progenitors for this event at the 90% confidence level. As a reference point, a compact binary progenitor with mass $1M_\odot < m_2 < 3M_\odot$ and $m_1 = 1.5M_\odot$ with $D < 5$ Mpc is excluded at 90% confidence. Moreover, this analysis exludes a binary neutron star progenitor out to 12 Mpc at the 50% level.

As more short, hard γ-ray bursts are observed and their distances measured, we can hope that one will be close enough to be detectable by earth-based gravitational-wave detectors. This could provide unambiguous evidence about the progenitors of these sources.

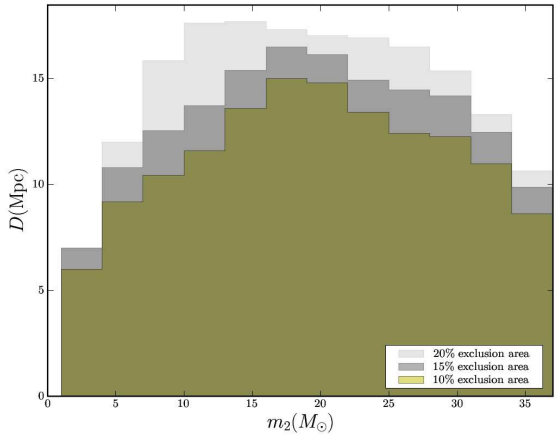

FIG. 3.— The probability as described in eq. (3) computed using the loudest event method where the injections are made only into the 180s segments immediately before and after the on-source time. The contours represent 20%, 15% and 10% exclusion limits. A compact binary progenitor is excluded in the darkest-shaded region at the 90% confidence level.

4. SEARCH FOR A GRAVITATIONAL WAVE BURST

To search for a gravitational wave burst associated with GRB070201 we have used LIGO's current baseline method for near-real time searches for gravitational wave bursts associated with GRB triggers **[ref GCN and IPN networks]**. A detailed description of the analysis method is presented elsewhere (LIGO Scientific Collaboration 2007b).

4.1. *Search method*

The burst search method is based on cross-correlating a pair of pre-conditioned datastreams from two different gravitational wave detectors. The pre-conditioning of the datastreams consists of whitening, phase-calibration, and band-passing from 40 Hz to 2000 Hz. The cross-correlation is calculated for short time series of equal length taken from the data streams of each detector. For discretely sampled time series s_1 and s_2, each containing n elements, the cross-correlation, cc, is defined as:

$$cc = \frac{\sum_{i=1}^{n}[s_1(i)-\mu_1][s_2(i)-\mu_2]}{\sqrt{\sum_{j=1}^{n}[s_1(j)-\mu_1]^2}\sqrt{\sum_{k=1}^{n}[s_2(k)-\mu_2]^2}} \quad (4)$$

where μ_1 and μ_2 are the corresponding means of s_1 and s_2. Possible values of this normalized cross-correlation range from -1 to +1, the minus sign corresponding to anti-correlation and the plus sign to correlation.

The measurement of the cross-correlation statistic proceeded as follows. Both 180-second on-source time series of H1 and H2 data were divided into time intervals (or cross-correlation windows) of length T_{ccw} seconds. Previous analyses have shown that using two windows, T_{ccw} = 25 ms and T_{ccw} = 100 ms, is sufficient to target short-duration signals lasting from $\sim$ 1 ms to $\sim$ 100 ms. The intervals were overlapped by half (i.e. $T_{ccw}/2$) to avoid missing a signal occurring near a boundary. The cross-correlation value, cc, was calculated for each H1-H2 interval pair and for both T_{ccw} cross-correlation window length. The largest cc is the strength measure of the most significant correlated candidate value within the 180 second long on-source segment. To estimate the significance of this loudest event, we use off-source data to measure the cross-correlation distribution of the background noise.

4.2. *Background estimation and search results*

Approximately 3 hours of data symmetrically distributed about the on-source segment was used to study the background. This off-source data was collected in the same lock stretch and is sufficiently close to the on-source time to reflect the background expected in the on-source time. The off-source data was divided into 180 second long segments, which correspond to the length of the on-source segment. The off-source segments were treated identically to the on-source segment.

The distribution of largest cc values in the absence of a signal was estimated for each cross-correlation window (T_{ccw} = 25 ms and T_{ccw} = 100 ms) by applying the method in Sec. 4.1 for all 180s long off-source data segments. To increase the off-source distribution statistics, time shifts between the H1 and H2 datastreams were also performed. The H1 datastream was shifted by multiples of 180 seconds relative to H2. Then two 180-second stretches from the two detectors were paired at each shift, making sure that two 180-second time stretches were paired only once. For both cross-correlation windows (T_{ccw}), the resulting off-source loudest event cc distribution was used to estimate the probability that background noise alone (i.e., without a GW signal) would produce a cc value larger than the largest cross-correlation found in the on-source segment.

Figure 4 shows the cumulative cross-correlation distribution for the T_{ccw} = 100 ms case. For the T_{ccw} = 25 ms time-window, the largest cross-correlation found in the on-source data was cc = 0.36. The probability of obtaining a cross-correlation value this large from noise alone is 0.58. For the T_{ccw} = 100 ms time-window, the largest cross-correlation found in the on-source data was cc = 0.15, and the probability for this cross-correlation value is 0.96. These results are, therefore, consistent with noise. We conclude that no gravitational wave burst associated with GRB070201 was detected by the search.

4.3. *Upper limits on the amplitude and energy of gravitational wave transients associated with GRB070201*

Since the analysis of the previous section showed no evidence for a gravitational wave burst, we set upper limits on the amplitude and energy of gravitational waves incident on

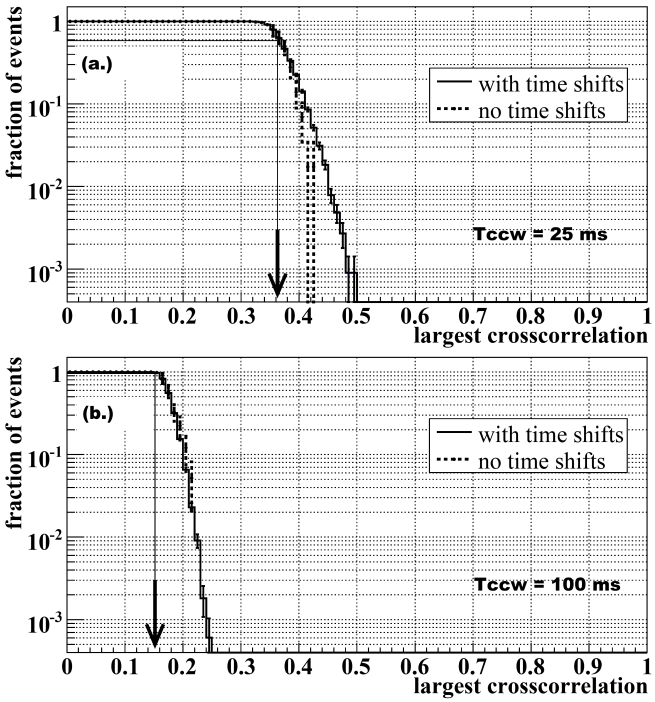

FIG. 4.— Cumulative distribution of measured cross-correlation values for the T_{ccw} = 25ms (a.) and T_{ccw} = 100ms (b.) cross-correlation windows. Both distributions with and without time shifts are shown, including the statistical errors. The arrows points to the largest cross-correlation found in the on-source segment.

the detectors during GRB070201. Denote the gravitational wave signal $h(t;h_{\rm rss})$ where

$$h_{\rm rss} = \sqrt{\int_{-\infty}^{\infty} (|h_+(t)|^2 + |h_\times(t)|^2)\, dt} \qquad (5)$$

is the root-sum-squared amplitude of the gravitational wave signal. To determine an upper limit, one needs the probability of measuring *cc* given the presence of a signal with $h_{\rm rss}$:

$$p[cc|h(t;h_{\rm rss})]\,. \qquad (6)$$

The search targets signals with duration $\lesssim 100$ ms. Within this class of signals, the sensitivity of the search has weak dependence on signal morphology; it depends primarily on the energy content and the frequency of the signal. Therefore, as long as the frequency and duration of the injected test waveforms match the theoretical predictions, we can work with the waveform of our choice. A class of waveforms called *sine-Gaussians* have become the standard benchmark for burst searches and were used to construct the probability distribution given in Eq. (6). The explicit formulae for $h_+(t)$ and $h_\times(t)$ are

$$h_+(t) = h_0 \sin(2\pi f_0 t) \exp\left(\frac{-(2\pi f_0 t)^2}{2Q^2}\right), \qquad (7)$$

$$h_\times(t) = h_0 \cos(2\pi f_0 t) \exp\left(\frac{-(2\pi f_0 t)^2}{2Q^2}\right), \qquad (8)$$

where f_0 is the central frequency, h_0 is the peak amplitude of each polarization, and Q is a dimensionless constant which represents roughly the number of cycles with which the waveform oscillates with more than half of the peak amplitude. Since the $h_+(t)$ and $h_\times(t)$ waveforms have the same amplitude, these simulated gravitational wave bursts are circularly polarized.

TABLE 1
90% AMPLITUDE UPPER LIMITS AND CORRESPONDING CHARACTERISTIC ENERGIES FROM SINE-GAUSSIAN WAVEFORM SIMULATIONS. THE TOP 6 ROWS ARE FOR T_{ccw}=25MS AND THE BOTTOM 6 ROWS REFER TO T_{ccw}=100MS. THESE NUMBERS ARE PRELIMINARY, BASED ON V3 CALIBRATION. ERRORS ARE NOT NOTED YET. E_{ISO} VALUES MUST BE RECOMPUTED.

sine-gaussian central frequency (Hz)	90% UL on $h_{\rm rss}$ ($\mathrm{Hz}^{-1/2}$)	characteristic $E_{\rm GW}^{\rm iso}$
100	1.75×10^{-21}	$\times 10$
150	1.03×10^{-21}	$\times 10$
250	1.09×10^{-21}	$\times 10$
554	1.93×10^{-21}	$\times 10$
1000	3.38×10^{-21}	$\times 10$
1850	6.03×10^{-21}	$\times 10$
100	1.60×10^{-21}	$\times 10$
150	1.03×10^{-21}	$\times 10$
250	1.16×10^{-21}	$\times 10$
554	2.07×10^{-21}	$\times 10$
1000	3.71×10^{-21}	$\times 10$
1850	6.68×10^{-21}	$\times 10$

We provide characteristic results for the case $Q = 8.9$. The measurement is carried out as follows. First, we choose a central frequency, f_0, and an $h_{\rm rss}$ value for the injected signal. From these parameters, we calculate $h(t)$ using Eq.(1), Eq.(5), Eq.(7) and Eq.(8). We then add the calibrated $h(t)$ to the on-source H1 and H2 data, choosing a random starting time within the segments. We then measure the largest value of cross-correlation, *cc*, following the same method described in section 4.1. Using the same $h_{\rm rss}$ values, we keep iterating the last two steps of the algorithm (randomizing a starting point and calculating the *cc* local maximum) until we have enough datapoints to determine the conditional probability $p(cc|h_{\rm rss})$. $p(cc|h_{\rm rss})$, for a given $h_{\rm rss}$ value, gives the probability of measuring *cc* within the local environment, corresponding to a signal injected in the on-source segment with a certain $h_{\rm rss}$ value. This probability, determined for different $h_{\rm rss}$ values and central frequencies, is then used to set a frequentist upper limit on $h_{\rm rss}$, given the largest cross-correlation found for the on-source segment in the actual search (see section **??**, LIGO Scientific Collaboration (2007b).

A number of systematic uncertainties enter into this analysis: calibration and Monte-Carlo statistics have the largest effects. These uncertainties are folded in by marginalizing over their effects in a manner similar to that described in Abbott et al. (2007).

The resulting 90% $h_{\rm rss}$ upper limits are given in Table 1 for circularly polarized sine-gaussians with different central frequencies and with Q = 8.9.

The upper limits on h_{rss} implied by the burst search can be translated into conventional astrophysical units of energy emitted in gravitational waves. The GW energy $E_{\rm GW}$ radiated by an isotropically-emitting source which is dominated by emission at a frequency f_0, is related to the $h_{\rm rss}$ received at distance D much less than the Hubble distance by

$$E_{\rm GW}^{\rm iso} \approx \frac{\pi^2 c^3}{G} D^2 f_0^2 h_{\rm rss}^2\,. \qquad (9)$$

Though this result assumes isotropic emission, it does not change significantly if the source emits slightly anisotropically, including when the emission is predominantly quadrap-

olar.

Based on the sensitivity of this burst search as summarized in Table 1, we estimate that a GW burst with characteristic frequency in the most sensitive frequency region of the LIGO detectors ($f \approx 150$Hz) from GRB070201 must have emitted less than approximately $3 \times 10^{-4} M_{\odot}$ in gravitational waves if the source was in M31. In terms of the SGR progenitor hypothesis, our experimental upper limit on E_{GW} is orders of magnitude above the $10^{45}\mathrm{erg}(D/770\mathrm{kpc})^2$ known to be emitted electromagnetically. And while present models for SGR bursts may differ substantially in their mechanism (de Freitas Pacheco 1998; Ioka 2001a,b; Horvath 2005), they suggest that no more than 10^{46}erg energy is released in the form of gravitational waves. Therefore, the upper limit achievable with the present detectors does not exclude these models of SGRs at the M31 distance.

5. DISCUSSION

We analysed the data from the LIGO H1 and H2 gravitational wave detectors, looking for gravitational wave signals associated with the GRB070201 event. No plausible gravitational-wave signals were identified above the noise background. Based on this search, a compact binary progenitor of GRB070201 located in M31 is excluded at the $> 99\%$ confidence. Due to the lack of detection and host galaxy association ambiguity, our search does not support or disprove an association between this GRB and binary mergers.

this section needs attention Our model independent search did not find correlated signatures, inconsisten with the noise, within the H1-H2 datastreams that could be related to GRB070201. Based on the sensitivity of our search and assuming isotropic gravitational-wave emission of the progenitor, an upper limit on the power emitted in gravitational waves by GRB070201 can determined. A gravitational wave with characteristic frequency within the most sensitive range of the LIGO detectors (f $\approx$ 150Hz) most probably emitted less than $E_{GW} < XXX \times 10^{50}$ erg within any 100ms long time interval inside the on-source region if the source is in M31. This limit on radiated power is comparable to the emitted power of some GRBs, however, in general it is significantly higher than the associated electromagnetic emission of this particular GRB. Therefore the unmodeled transient search only weakly constrains other possible source candidate models for a short GRB in M31, such as a magnetar-driven burst comparable to SGR1806-20.

As gravitational-wave observations continue and the sensitivity of the instruments continues to improve, we look forward to the scientific pay-off that combined electromagnetic and gravitational observing campaigns can bring.

6. ACKNOWLEDGMENTS

We are indebted to the observers of the electromagnetic event and the GCN network for providing us with valuable data and real time information.

The authors gratefully acknowledge the support of the United States National Science Foundation for the construction and operation of the LIGO Laboratory and the Particle Physics and Astronomy Research Council of the United Kingdom, the Max-Planck-Society and the State of Niedersachsen/Germany for support of the construction and operation of the GEO600 detector. The authors also gratefully acknowledge the support of the research by these agencies and by the Australian Research Council, the Natural Sciences and Engineering Research Council of Canada, the Council of Scientific and Industrial Research of India, the Department of Science and Technology of India, the Spanish Ministerio de Educacion y Ciencia, The National Aeronautics and Space Administration, the John Simon Guggenheim Foundation, the Alexander von Humboldt Foundation, the Leverhulme Trust, the David and Lucile Packard Foundation, the Research Corporation, the Alfred P. Sloan Foundation and Columbia University in the City of New York.

REFERENCES

T. Piran, Reviews of Modern Physics **76**, 1143 (2005), URL http://adsabs.harvard.edu/cgi-bin/nph-bib_query?bibcode=2005RvMP...76.1143P&db_key=AST&high=432eb689bf01702.

P. Meszaros, Annual Review of Astronomy and Astrophysics **40**, 137 (2002), URL http://adsabs.harvard.edu/cgi-bin/nph-bib_query?bibcode=2002ARA%26A..40..137M&db_key=AST&high=432eb689bf01702.

R. W. Klebesadel, I. B. Strong, and R. A. Olson, ApJ **182**, L85+ (1973).

C. A. Meegan, G. J. Fishman, R. B. Wilson, J. M. Horack, M. N. Brock, W. S. Paciesas, G. N. Pendleton, and C. Kouveliotou, Nature **355**, 143 (1992).

W. S. Paciesas, C. A. Meegan, G. N. Pendleton, M. S. Briggs, C. Kouveliotou, T. M. Koshut, J. P. Lestrade, M. L. McCollough, J. J. Brainerd, J. Hakkila, et al., ApJS **122**, 465 (1999), arXiv:astro-ph/9903205.

F. Frontera, L. Amati, E. Costa, J. M. Muller, E. Pian, L. Piro, P. Soffitta, M. Tavani, A. Castro-Tirado, D. Dal Fiume, et al., ApJS **127**, 59 (2000), arXiv:astro-ph/9911228.

E. P. Mazets and S. V. Golenetskii, Ap&SS **75**, 47 (1981).

N. Gehrels, G. Chincarini, P. Giommi, K. O. Mason, J. A. Nousek, A. A. Wells, N. E. White, S. D. Barthelmy, D. N. Burrows, L. R. Cominsky, et al., ApJ **611**, 1005 (2004), arXiv:astro-ph/0405233.

C. Kouveliotou, C. A. Meegan, G. J. Fishman, N. P. Bhat, M. S. Briggs, T. M. Koshut, W. S. Paciesas, and G. N. Pendleton, ApJ **413**, L101 (1993).

N. Gehrels, J. P. Norris, S. D. Barthelmy, J. Granot, Y. Kaneko, C. Kouveliotou, C. B. Markwardt, P. Mészáros, E. Nakar, J. A. Nousek, et al., Nature **444**, 1044 (2006).

D. Watson, J. N. Reeves, J. Hjorth, J. P. U. Fynbo, P. Jakobsson, K. Pedersen, J. Sollerman, J. M. Castro Cerón, S. McBreen, and S. Foley, ApJ **637**, L69 (2006).

P. Jakobsson, A. Levan, J. P. U. Fynbo, R. Priddey, J. Hjorth, N. Tanvir, D. Watson, B. L. Jensen, J. Sollerman, P. Natarajan, et al., A&A **447**, 897 (2006).

S. Campana et al., Nature **442**, 1008 (2006), astro-ph/0603279.

J. Hjorth et al., Nature. **423**, 847 (2003), astro-ph/0306347.

T. J. Galama et al., Nature **395**, 670 (1998), astro-ph/9806175.

E. Nakar, A. Gal-Yam, T. Piran, and D. B. Fox, ApJ **640**, 849 (2006).

K. Hurley, S. E. Boggs, D. M. Smith, R. C. Duncan, R. Lin, A. Zoglauer, S. Krucker, G. Hurford, H. Hudson, C. Wigger, et al., Nature **434**, 1098 (2005), arXiv:astro-ph/0502329.

E. Nakar, ArXiv Astrophysics e-prints (2007).

B. Abbott and et al, Phys. Rev. D **72**, 042002 (2005).

C. S. Kochanek and T. Piran, ApJ **417**, L17+ (1993).

LIGO Scientific Collaboration, Classical and Quantum Gravity **23**, 29 (2006).

LIGO Scientific Collaboration, Phys. Rev. D **72**, 082001 (2005).

L. S. Finn, B. Krishnan, and P. J. Sutton, ApJ **607**, 384 (2004).

S. Golenetskii, R. Aptekar, E. Mazets, V. Pal'Shin, D. Frederiks, T. Cline, A. von Kienlin, G. Lichti, A. Rau, D. Gotz, et al., GRB Coordinates Network **6088**, 1 (2007a).

D. A. Perley and J. S. Bloom, GRB Coordinates Network **6091**, 1 (2007).

V. Pal'Shin, GRB Coordinates Network **6098**, 1 (2007).

S. Golenetskii, R. Aptekar, E. Mazets, V. Pal'Shin, D. Frederiks, and T. Cline, GRB Coordinates Network **6094**, 1 (2007b).

E. Berger, Submitted to ApJ (astro-ph/0702694) (2007), URL http://xxx.lanl.gov/abs/astro-ph/0702694.

B. Abbott et al. (LIGO Scientific Collaboration), Nucl. Instrum. Methods **A517**, 154 (2004).

F. Acernese, P. Amico, M. Alshourbagy, F. Antonucci, S. Aoudia, S. Avino, D. Babusci, G. Ballardin, F. Barone, L. Barsotti, et al., Classical and Quantum Gravity **23**, S635 (2006), URL http://stacks.iop.org/0264-9381/23/S635.

P. Grandclement, V. Kalogera, and A. Vecchio, Phys. Rev. D **67**, 042003 (2003).

LIGO Scientific Collaboration, XX **XX**, XX (XXX).

B. Abbott et al. (LIGO Scientific Collaboration), Phys. Rev. D **72**, 082001 (2005a), web location:gr-qc/0505041.

B. Abbott et al. (LIGO Scientific Collaboration), Phys. Rev. D **73**, 062001 (2006).
B. Abbott et al. (LIGO Scientific Collaboration), Phys. Rev. D **72**, 082002 (2005b), gr-qc/0505042.
B. Abbott et al. (LIGO Scientific Collaboration), gr-qc (2007), arXiv:0704.3368.
LIGO Scientific Collaboration, In preparation (2007a).
L. A. Wainstein and V. D. Zubakov, Extraction of signals from noise (Prentice-Hall, Englewood Cliffs, NJ, 1962).
L. Blanchet, T. Damour, and B. R. Iyer, Phys. Rev. D **51**, 5360 (1995).
M. Vallisneri, Phys. Rev. Lett. **84**, 3519 (2000), gr-qc/9912026.
E. Rantsiou, S. Kobayashi, P. Laguna, and F. Rasio (2007), astro-ph/0703599.
B. A. Allen, W. G. Anderson, P. R. Brady, D. A. Brown, and J. D. E. Creighton (2005), gr-qc/0509116.
B. Allen, Phys. Rev. D **71**, 062001 (2005).
A. Rodriguez, Master's thesis, Louisiana State University (2007), URL http://www.ligo.caltech.edu/docs/T/P070056-00.pdf.
K. S. Thorne, Astrophys. J. **191**, 507 (1974).
G. B. Cook, S. L. Shapiro, and S. A. Teukolsky, Astrophys. J. **424**, 823 (1994).
A. M. Soderberg, E. Berger, M. Kasliwal, D. A. Frail, P. A. Price, B. P. Schmidt, S. R. Kulkarni, D. B. Fox, S. B. Cenko, A. Gal-Yam, et al., ApJ **650**, 261 (2006).
D. Grupe, D. N. Burrows, S. K. Patel, C. Kouveliotou, B. Zhang, P. Mészáros, R. A. M. Wijers, and N. Gehrels, ApJ **653**, 462 (2006).
LIGO Scientific Collaboration, LIGO-P060024-05-Z (To be submitted to Phys. Rev. D) (2007b).
J. A. de Freitas Pacheco, Astronomy and Astrophysics **336**, 397 (1998), astro-ph/9805321.
K. Ioka, MNRAS **327**, 639 (2001a), arXiv:astro-ph/0009327.
K. Ioka, Monthly Notices of the RAS **327**, 639 (2001b), astro-ph/0009327.
J. E. Horvath, Modern Physics Letters A **20**, 2799 (2005).